Correlation Effects in the Two-Dimensional Vibrational Spectroscopy of Coupled Vibrations

N. Demirdöven, M. Khalil, O. Golonzka, and A. Tokmakoff*

Department of Chemistry, Massachusetts Institute of Technology, Cambridge, Massachusetts 02139

Received: March 29, 2001; In Final Form: June 17, 2001

Correlated energy shifts in the spectral broadening of coupled vibrational transitions are shown to have clear signatures in infrared two-dimensional dispersed vibrational echo (DVE) spectroscopy. A model that includes correlation effects through a correlation coefficient (ρ) for a bivariate distribution is used to describe two-dimensional experiments on the coupled carbonyl stretches of $Rh(CO)_2(C_5H_7O_2)$ (or RDC) in chloroform. Signatures of correlated ($0 < \rho < +1$) and anticorrelated ($-1 < \rho < 0$) broadening in DVE experiments manifest themselves in the depth of modulation of the signal and the magnitude of the echo peak shift. For the case of RDC, the broadening is highly correlated ($\rho = 0.9$) and can be explained in terms of the solvent-induced modulation of the Rh electron density.

I. Introduction

Nonlinear spectroscopies have proven to be successful at characterizing the spectral broadening of electronic and vibrational transitions in solution arising from inter- and intramolecular interactions.[1] Such methods have advanced to the point where system−bath interactions can be described over multiple time scales.[2,3] Increasingly, such methods are being applied to the study of systems with multiple coordinates in which the interactions between these coordinates and their environments are of interest. This is particularly the case with two-dimensional (2D) spectroscopies,[4] where coupling between system coordinates is observed as the formation of cross-peaks in a 2D spectrum,[5−8] and spectral broadening is characterized by the 2D line shape.[9−13]

The sensitivity of 2D spectroscopies to couplings between coordinates implies that they will also be sensitive to static and dynamic correlations in their energies. In particular, for two coordinates interacting with one another and a bath, one can imagine interactions that would lead to certain types of correlated fluctuations in their energies. The energies of the two coordinates could fluctuate either in a purely random manner, in a correlated manner where the fluctuations of both states are equivalent, or in an anticorrelated manner in which they are precisely opposite. Such correlation effects can be explained by the disorder in the energies of the coordinates or the coupling between them. In this paper, we show that the 2D infrared (IR) spectroscopy of coupled vibrations based on vibrational echo experiments is sensitive to these correlation effects and can therefore be used to gain detailed insight into the microscopic mechanisms of vibrational couplings and vibrational solvation dynamics.

The influence of correlated broadening on spectroscopic transitions has been most thoroughly investigated for electronic chromophore aggregates. Pioneering work in the treatment of site energy disorder on J-aggregates has shown that correlated disorder profoundly affects the absorption line shapes of linear and cyclic aggregates.[14−17] Knoester suggested that linear absorption spectra do not contain sufficient information to determine the magnitude of site disorder and the degree of correlation independently; Knoester therefore proposed a two-color pump−probe spectroscopy as a method for probing these parameters.[18−20] The influence of correlated disorder on the nonlinear optical response of molecular aggregates was also studied by Chernyak et al.[21,22]

The sensitivity of nonlinear spectroscopies to correlation effects in other structurally disordered systems has been noted for some time. Photochemical hole-burning measurements on dye molecules[23,24] and difference-frequency-mixing theories[25] demonstrated the effect of the correlation of inhomogeneously broadened transitions on the spectral line widths. The influence of correlated disorder on photon echo experiments in semiconductor quantum wells has also been shown to be significant.[26−28] More recently, Yang and Fleming have discussed how nonlinear techniques can help describe intermolecular energy-transfer processes in disordered systems with correlation in the transition energies.[29] Also, the signatures of diagonal and off-diagonal disorder in the 2D IR spectroscopy of coupled vibrations have been described.[30] Correlated fluctuations between fundamental and overtone vibrational transition frequencies have been addressed for fifth-order Raman spectroscopy as well.[31]

In this paper we investigate correlation effects in the spectral broadening of two coupled vibrational coordinates using dispersed vibrational echo (DVE) spectroscopy. The results presented here are modeled using the nonlinear response from two coupled vibrations which are ensemble averaged over a bivariate distribution that incorporates correlation between the transition frequencies. The degree of correlation in the energy shifts of the two vibrations is quantified through a correlation coefficient. The experimental data are shown to have distinct signatures of the degree of correlation: the depth of the modulation of beats on the signal and the magnitude of the echo peak shift. Experiments on a metal dicarbonyl in chloroform show clear evidence for strongly correlated spectral broadening of the two carbonyl-stretching transitions. These results parallel the recent work of Fayer and co-workers who have also applied 2D DVE spectroscopy to investigate correlated inhomogeneous broadening.[32,33]

II. Experimental Section

Two-dimensional dispersed vibrational echo (2D DVE) spectroscopy is a resonant third-order method that monitors the

10.1021/jp011215d CCC: $20.00
Published on Web 08/02/2001

evolution of vibrational coherences as a function of two independent time periods τ_1 and τ_3.[8,34] The third-order nonlinear signal $E_s^{(3)}(k_s)$ is generated by the interaction of the sample with a sequence of three-pulsed infrared laser fields $E_1(k_1)$, $E_2(k_2)$, and $E_3(k_3)$ that radiate the signal into the phase-matching direction $k_s = -k_1 + k_2 + k_3$. Vibrational coherences initially created by the first field are acted on by the remaining fields after a delay τ_1, leading to either the rephasing of the initial coherence, further excitation of the vibration, or the transfer of the coherence to a coupled vibration. The frequency components of the signal radiated from the sample during τ_3 represent the second dimension in the experiment and reflect the final coherent state of the system. For two coupled vibrations, the signal must be described in terms of a six-level system consisting of the ground state and singly and doubly excited states. These states lead to a response expressed as a sum over 14 different nonlinear processes that satisfy the phase-matching condition.[35,36] Two-dimensional dispersed electronic and vibrational photon echo experiments such as these have been used to study electronic dephasing in dye molecules,[37] the interaction between carriers in semiconductors,[27,28,38] and vibrational inhomogeneous broadening.[8]

The experimental apparatus is described in detail in the literature.[39] Briefly, we used 90 fs mid-IR pulses ($\lambda = 4.9$ mm; $n = 2050$ cm^{-1}) generated by difference frequency mixing of the signal ($\lambda = 1.3$ mm) and idler ($\lambda = 1.9$ mm) outputs of a BBO optical parametric amplifier in an $AgGaS_2$ crystal. The IR beam was split into three pulses and focused into the sample ($\omega_0 = 150$ mm) in a standard "boxcar" configuration using a 10-cm parabolic mirror. The timing between the first pulse and the time-coincident second and third fields τ_1 was controlled with a 0.1 μm stepper motor. The nonlinear signal emitted from the sample was collimated by a second parabolic mirror, dispersed into its Fourier components ω_3 in a 190-mm grating monochromator, and then detected after exiting the exit slit by a single-element HgCdTe detector. A 2D data set was constructed by collecting signal amplitude data in 2 cm^{-1} intervals in ω_3 and 30 fs steps in τ_1. The polarization of each field in the experiment was controlled with wire-grid polarizers. The data presented here were taken in the all-parallel polarization geometry R_{zzzz}.

Two-dimensional DVE experiments have been performed on the anharmonically coupled symmetric (*s*) and asymmetric (*a*) carbonyl ($-C\equiv O$) stretching modes of acetylacetonato-dicarbonylrhodium(I), $Rh(CO)_2(C_5H_7O_2)$, or RDC. In addition to the fundamental transitions of *a* and *s* modes, transitions of the singly excited states into their corresponding overtone and combination bands are also resonant with the pulse spectrum. Hence, the 2D DVE experiment is sensitive to six resonances.[7] The FT-IR spectrum of RDC (Fluka) dissolved in spectroscopic-grade chloroform (Aldrich) shows two fundamental transitions at $\omega_a = 2015$ cm^{-1} and $\omega_s = 2084$ cm^{-1} with FWHM line widths of $\Delta\omega_a = 14.6$ cm^{-1} and $\Delta\omega_a = 9.3$ cm^{-1}. The anharmonic shifts determined from the FT-IR overtone and combination spectrum are $\Delta_{aa} = \Delta_{ss} = 11$ cm^{-1} and $\Delta_{as} = 24$ cm^{-1}, respectively. These are in accordance with the previously published results of pump−probe experiments.[40] Here we refer to the resonances between one- and two-quantum states as overtones and combination transitions, although these terms are used for transitions between zero- and two-quantum states in traditional vibrational spectroscopy. The experiments were performed at room temperature with a 0.01 M sample held in a CaF_2 cell with a 0.2 mm path length corresponding to a peak optical density of 0.5.

III. Theory

Here we derive an analytical form for the total third-order nonlinear signal for the 2D DVE experiment $S(\tau_1,\omega_3)$ from two coupled vibrational modes. The nonlinear response is obtained by ensemble averaging the individual contributions to the total third-order nonlinear polarization over a bivariate distribution function that includes the effects of correlated frequency shifts for the two coordinates.

Correlation of Spectrally Broadened Transitions. For a particular molecular vibrational transition *m*, its frequency ω_m can be defined as

$$\omega_m = \omega_m^o + \Delta\omega_m \tag{1}$$

where ω_m^o is the ensemble-averaged transition frequency and $\Delta\omega_m$ is the frequency shift for an individual transition relative to the mean. The shift $\Delta\omega_m$ is a random variable that characterizes the spectral distribution. It is generally time dependent;[2,41] however, here we will work in the slow modulation limit, taking $\Delta\omega_m$ to be static. When we introduce a second transition *n*, even if the statistics for $\Delta\omega_m$ are treated as being random, microscopic interactions between these coordinates may lead to a correlation between individual transition shifts $\Delta\omega_n$ and $\Delta\omega_m$. We can formulate the statistical interdependence between $\Delta\omega_m$ and $\Delta\omega_n$ through a Normal joint probability distribution function (PDF) that can be written as

$$G(\Delta\omega_m,\Delta\omega_n) = \frac{1}{2\pi\sqrt{1-\rho^2}\sigma_m\sigma_n} \times \exp\left[-\frac{1}{2(1-\rho^2)}\left(\frac{\Delta\omega_m^2}{\sigma_m^2} - 2\rho\frac{\Delta\omega_m\Delta\omega_n}{\sigma_m\sigma_n} + \frac{\Delta\omega_n^2}{\sigma_n^2}\right)\right] \tag{2}$$

where σ_i is the width of the transition frequency distribution around the central frequency ω_i^o and ρ is the correlation coefficient, which is defined as the normalized covariance of the random variables $\Delta\omega_n$ and $\Delta\omega_m$:[42]

$$\rho = \frac{\langle\Delta\omega_m\Delta\omega_n\rangle}{\sigma_m\sigma_n} \tag{3}$$

Here $\langle ... \rangle$ denotes a joint average of the individual transitions over the ensemble. Equation 3 shows that ρ can take on values between -1 and $+1$, where the magnitude of ρ reflects the degree of correlation of the individual frequencies. For the limiting case of $\rho = \pm 1$, a complete linear dependence exists between the variables $\Delta\omega_m$ and $\Delta\omega_n$ described by

$$\Delta\omega_n = \pm\frac{\sigma_n}{\sigma_m}\Delta\omega_m \tag{4}$$

that, in the case where $\sigma_m = \sigma_n$, leads to

$$\omega_m \mp \omega_n = \omega_n^o \mp \omega_m^o \tag{5}$$

The difference of the two transition frequencies for a particular molecule is constant when $\rho = +1$, whereas their sum is constant when $\rho = -1$. These limiting cases, illustrated in Figure 1, are termed correlated and anticorrelated broadening. In this limit, $G(\Delta\omega_m,\Delta\omega_n)$ reduces to a product of a univariate Normal Gaussian PDF and a δ function, showing that each value of $\Delta\omega_m$ dictates a single value of $\Delta\omega_n$. For any other value, the magnitude of ρ represents the degree to which the frequencies are correlated. Statistical independence requires that $\rho = 0$, for

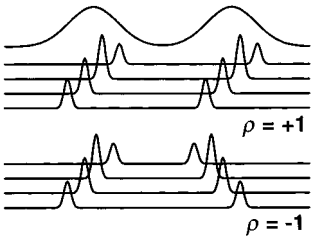

Figure 1. Schematic representation of perfectly correlated ($\rho = +1$) and perfectly anticorrelated ($\rho = -1$) broadening of the absorption lines of two coupled vibrations.

which $G(\Delta\omega_m,\Delta\omega_n)$ becomes a product of two independent univariate Normal Gaussian distributions.

Response Functions. The third-order nonlinear vibrational response from a pair of vibrational coordinates requires the consideration of the six lowest vibrational states for the coupled system.[7,35,36] For the current case, we used the optical Bloch formalism, including orientational relaxation, for which the nonlinear response as a function of the two-time variables describing 2D DVE experiments is written for a given polarization condition *ijkl* as

$$\mathcal{R}_{ijkl}(\tau_1,\tau_3) = \sum_{m,n=a,s} \exp[i(\omega_m^o + \Delta\omega_m)\tau_1 - \Lambda_{m,0}\tau_1] \times \exp[-i(\omega_n^o + \Delta\omega_n)\tau_3 - \Lambda_{n,0}\tau_3] \times [(c_{ijkl}^{mmnn} + c_{ijkl}^{mnmn})|\mu_{m,0}|^2|\mu_{n,0}|^2 - e^{i\Delta_{mn}\tau_3}(c_{ijkl}^{mmnn}|\mu_{m,0}|^2|\mu_{mn,m}|^2_{m\neq n} + c_{ijkl}^{mnmn}\mu_{m,0}\mu_{n,0}\mu_{mn,n}\mu_{m,mn})] \quad (6)$$

where $c_{ijkl}^{\nu\kappa\chi\lambda}$ is a tensorial orientational factor that is dependent on the polarization conditions *ijkl* and the vibrational interaction pathway $\nu\kappa\chi\lambda$. In the present 2D DVE experiments with parallel excitation polarization ($\mathcal{R}_{zzzz}$), $c_{zzzz}^{mmmm} = 1/5$ and $c_{zzzz}^{mmnn} = c_{zzzz}^{mnmn} = 1/15$.[35] In eq 9, $\mu_{m,0}$, $\mu_{mm,m}$, and $\mu_{nm,m}$ are the transition dipole-moment matrix elements of the fundamental ($|00\rangle \rightarrow |10\rangle$), overtone ($|10\rangle \rightarrow |20\rangle$), and combination ($|10\rangle \rightarrow |11\rangle$) transitions, respectively, for the vibration *m*. For the summation, the fundamental overtone and combination transitions of the asymmetric vibration are labeled *a*, and the fundamental overtone and combination transitions of the symmetric vibration are labeled *s*. The damping of vibrational coherences is described as

$$\Lambda_{i,j} = \Gamma_{i,j} + 2D_{or} \quad (7)$$

where Γ may have contributions from isotropic pure dephasing and vibrational lifetime and reorientation of the molecule through small-angle diffusion with a diffusion constant D_{or}. Anharmonic shifts of the overtone ($m = n$) and combination ($m \neq n$) transitions relative to the fundamental are represented by Δ_{mn}. In modeling the distribution, we have taken these anharmonic shifts as constant values, implying that they are fully correlated with the fundamentals.

The ensemble-averaged response function is obtained by integrating eq 6 over the joint PDF

$$R(\tau_1,\tau_3) = \int_{-\infty}^{\infty} d(\Delta\omega_n) \int_{-\infty}^{\infty} d(\Delta\omega_m) G(\Delta\omega_m,\Delta\omega_n) \mathcal{R}(\tau_1,\tau_3) \quad (8)$$

To describe the 2D DVE signal, the total response is obtained by the Fourier−Laplace transformation along τ_3

$$R(\tau_1,\omega_3) = \int_0^{\infty} d\tau_3 \exp(i\omega_3\tau_3) R(\tau_1,\tau_3)$$

for which we obtain the following analytical expression:

$$R_{zzzz}(\tau_1,\omega_3) = \sum_{m,n=a,s} 2c_{zzzz}^{mmnn}|\mu|^4 \times \exp\left[i\omega_m^o\tau_1 - i(\omega_3 - \omega_n^o)\frac{(\Lambda_{n,0} - \rho_{mn}\sigma_m\sigma_n\tau_1)}{\sigma_n^2}\right] \times \exp\left[-\left(\Lambda_{m,0} + \Lambda_{n,0}\rho_{mn}\frac{\sigma_m}{\sigma_n}\right)\tau_1\right] \exp\left[-(1-\rho_{mn}^2)\frac{\sigma_m^2\tau_1^2}{2} - \frac{\Lambda_{n,0}^2}{2\sigma_n^2}\right] \times \left\{\exp\left[-\frac{(\omega_3 - \omega_n^o)^2}{2\sigma_n^2}\right] \times erfc\left[\frac{-i(\omega_3 - \omega_n^o) + (\Lambda_{n,0} - \rho_{mn}\sigma_m\sigma_n\tau_1)}{\sqrt{2}\sigma_n}\right] - \exp\left[-\frac{(\omega_3 - \omega_n^o + \Delta_{mn})^2}{2\sigma_n^2}\right] \times \exp\left[-i\Delta_{mn}\frac{(\Lambda_{n,0} - \rho_{mn}\sigma_m\sigma_n\tau_1)}{\sigma_n^2}\right] \times erfc\left[\frac{-i(\omega_3 - \omega_n^o + \Delta_{mn}) + (\Lambda_{n,0} - \rho_{mn}\sigma_m\sigma_n\tau_1)}{\sqrt{2}\sigma_n}\right]\right\} \quad (9)$$

Here, $\rho_{mn} = 1$ for $m = n$, and $\rho_{mn} = \rho$ for $m \neq n$. On the basis of the dipole amplitudes in other studies of RDC,[7] we have taken the transition dipoles for fundamental *a* and *s* vibrations to be equal and all the other transition dipoles between the one- and two-quantum states to be scaled harmonically, i.e., $\mu_{a,0} = \mu_{s,0} = \mu$, $\mu_{as,a} = \mu_{as,s} = \mu$, and $\mu_{aa,a} = \mu_{ss,s} = \sqrt{2}\mu$.

Equation 9 describes the total response for a six-level system arising from two inhomogeneously broadened vibrational transitions. The primary assumptions made about the dynamics of the system are (i) correlated broadening described by a bivariate Normal distribution with a correlation coefficient ρ, (ii) constant anharmonicity parameters, and (iii) identical dephasing dynamics of a particular transition for all members of the ensemble. Thus, the dephasing of the overtone and combination bands have been set equal to those of the corresponding fundamentals; more generally, this is not required. Finally, the signal detected in a 2D DVE experiment is calculated in the short pulse limit by taking the absolute value square of the total response function, $S(\tau_1,\omega_3) \propto |R(\tau_1,\omega_3)|^2$.

Figure 2 shows the calculated 2D DVE signals of two coupled vibrations for the two limiting cases of the perfectly correlated ($\rho = +1$) and perfectly anticorrelated ($\rho = -1$) broadening. All other parameters in eq 9 have been held constant and are chosen to reflect the dynamics of the symmetric and asymmetric carbonyl stretches of RDC in $CHCl_3$, for which $\sigma_i \approx \Delta_i > \Lambda_i$. Figure 2 shows distinct signatures of correlated and anticorrelated broadening, which are reflected in the dispersed signal by polarization beats along τ_1 at roughly the splitting between the fundamental transitions. For a given fundamental detection frequency ω_3, these oscillations originate from the interference between two types of subensembles that differ in their field-induced vibrational interaction pathways: (i) those for which the initially excited vibrational coordinate was the same as the

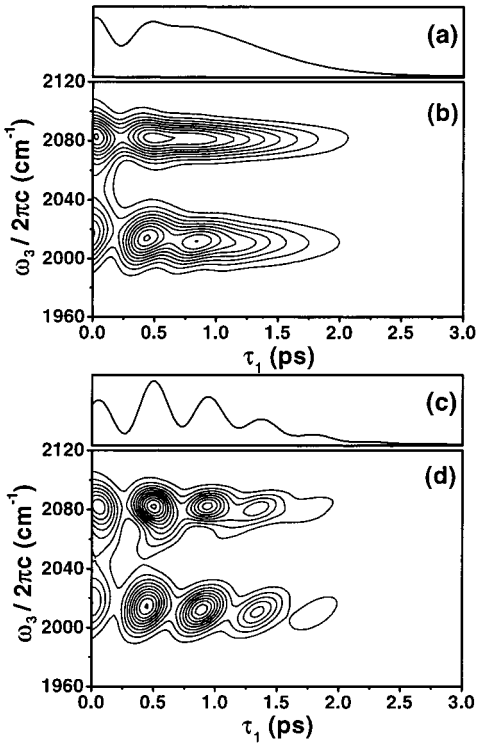

Figure 2. Simulated 2D DVE spectra of RDC in $CHCl_3$ for the two limiting cases of (b) $r = -1$ and (d) $r = +1$ using eq 9. Slices from the simulation along $\omega_3 = 2084$ cm^{-1} shown in (a) and (c) illustrate the magnitude of the echo peak shift for $r = -1$ and $r = +1$, respectively. The remaining parameters used in the calculation are identical for both simulations ($\sigma_a = 11.9$ cm^{-1}, $\sigma_s = 7.5$ cm^{-1}, $1/\Lambda_a = 1.8$ ps, and $1/\Lambda_s = 1.8$ ps).

detected coordinate ($\omega_1 = \omega_3$) and (ii) those for which the other coordinate was initially excited and the later pulses in the echo sequence transferred coherence to ω_3.[8]

In the case of perfect correlation, the beats almost completely modulate the signal along τ_1, and a slight frequency dependence to the oscillation period is observed near each of the fundamentals. The ω_3-dependent beat frequency is observed as diagonally tilted beat contours in the 2D signal. In the case of purely anticorrelated broadening, the overall-signal decay times remain approximately the same; however, the depth of the modulation of beats is dramatically reduced to the point of vanishing in the tail of the decays. Additionally, in the case of correlated broadening, a peak shift of the signal away from $\tau_1 = 0$ is observed, whereas no peak shift is observed in the anticorrelated case. As seen from eq 9, the amplitude and lifetime of the beats strongly depend on the correlation coefficient and do not necessarily reflect the lifetime of the individual coherences. This point should be considered when deriving dynamical information from experimental photon echo decay constants on multilevel systems. Similar issues may arise in photon echo peak shift (3PEPS) measurements on multilevel systems, where the magnitude of the peak shift will reflect correlation effects such as the strength of coupling between states.[43,44]

The influence of ρ on the magnitude of the echo peak shift during τ_1 reflects the manner in which correlated broadening influences the rephasing ability of vibrational echo experiments on multilevel systems.[21] In traditional echo experiments on two-level systems, slowly varying or inhomogeneous contributions to the dephasing dynamics during τ_1 are rephased during τ_3. The degree of rephasing influences the magnitude of the echo peak shift. For echo experiments on multilevel systems, the system may evolve on two different transitions during the two time periods. Therefore, the rephasing ability for certain field interaction sequences depends on the phase relationship between the phase acquired in one coherence during τ_1, $e^{i\omega_m\tau_1}$, and the phase reversed in another during τ_3, $e^{-i\omega_n\tau_3}$. This in turn will depend on the correlation between the frequency of the two coherences ω_m and ω_n. If perfect correlation exists ($\rho = +1$), the phase acquired during τ_1 can be exactly rephased during τ_3, leading to a large peak shift. In the case of zero correlation ($\rho = 0$), no phase relationship exists between the coherences, and rephasing is suppressed. For anticorrelated broadening, the inverse frequency-shift relationship between the two transitions leads to additional dephasing during τ_3 and enhanced suppression of the peak shift in the echo experiment. However, for anticorrelated broadening, we expect that rephasing, and the accompanying peak shift, will be recovered with a dispersed transient-grating experiment.

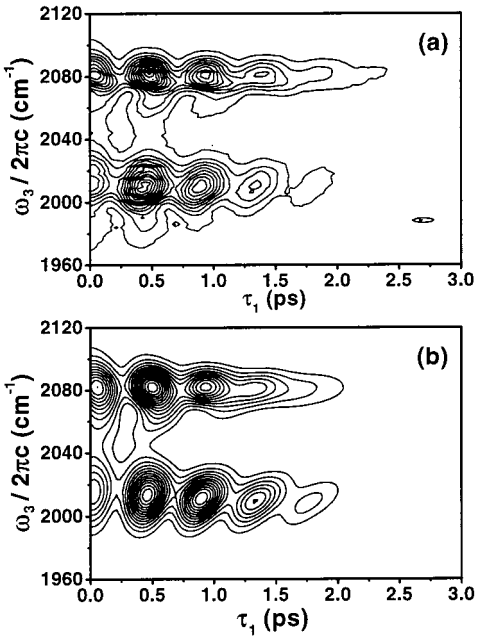

Figure 3. (a) Experimental 2D DVE signals of RDC in $CHCl_3$ and (b) a calculation obtained from the nonlinear least-squares fit to the experimental data ($\sigma_a = 11.9$ cm^{-1}, $\sigma_s = 7.5$ cm^{-1}, $1/\Lambda_a = 1.8$ ps, and $1/\Lambda_s = 1.8$ ps). See the text for details.

IV. Results and Discussion

Figure 3a shows the 2D DVE spectrum of the carbonyl-stretching region of RDC in chloroform. The signal along τ_1 is deeply modulated with a period of ca. 450 fs, corresponding to the frequency separation of the fundamentals (70 cm^{-1}). A large peak shift of the signal maximum away from $\tau_1 = 0$ is observed for both fundamentals, and a frequency dependence of this peak shift results in the tilted shapes of the contours. These are all clear signatures of strongly correlated spectral broadening. The decay of the signal from the asymmetric and symmetric vibrations occurs on different time scales. In addition, we note that only two features are resolved along ω_3, implying that signals radiated from the fundamental and overtone transitions overlap, so that $\sigma_i \approx \Delta_i$. Signals radiated from the combination band are discerned as the twisting of the signal contours in the wings near $\omega_3 = 2060$ and 1990 cm^{-1}.

Figure 3b gives a fit of the experimental spectrum to the expression in eq 9 using a nonlinear least-squares-fitting routing based on a modified Levenberg−Marquart algorithm and a finite-difference Jacobian. The obtained best-fit parameters are

given in the figure caption. The fit yields a correlation coefficient of $\rho = 0.9 \pm 0.1$, implying a highly correlated broadening of the two carbonyl-stretching transitions. The dephasing times of the asymmetric and symmetric modes are approximately 1.8 ps, which appear to be unreasonably long in comparison to the 3-ps time scale over which the signal vanishes. Equation 9 shows that the observed exponential decay constant of a given frequency ω_3 is affected by the actual dephasing constants, the extent of correlation, and the relative magnitude of the broadening for transitions *m* and *n*. This point was also demonstrated in a related theoretical study by Cundiff.[26] Thus, obtaining information on dephasing dynamics by fitting a simple exponential to the experimental data may be misleading. Correlation effects and the relative magnitude of the broadening for different transitions must be considered. Our best-fit results are in parallel with this prediction. The predicted widths of the frequency distribution for the asymmetric and symmetric vibrations are 11.7 and 7.4 cm^{-1}, respectively. Thus, the value of σ/Λ is ca. 3 for these transitions, which approaches the slow modulation limit in accordance with our treatment.

The model presented here allows the ensemble-averaged correlation coefficient ρ of the frequency modulation of two transitions to be determined. The magnitude of ρ will depend on the particular details of the coupling between the two vibrations and specific solute−solvent interactions at the microscopic level. In the case of RDC, we have described elsewhere the interaction potential between the two carbonyl groups in terms of a bilinear coupling constant V_{ij} and a diagonal cubic anharmonicity g_{iii}.[39]

$$V(Q_1,Q_2) = \frac{1}{2}\hbar\omega_1 Q_1^2 + \frac{1}{2}\hbar\omega_2 Q_2^2 + V_{12}Q_1Q_2 + \frac{1}{6}(g_{111}Q_1^3 + g_{222}Q_2^3) \quad (10)$$

where Q_i is the reduced local vibrational coordinate representing the stretching motion of one carbonyl group. In such a model, if there is a distribution of bilinear coupling parameters V_{ij} (off-diagonal disorder), anticorrelated broadening will be observed since the coupling strength dictates the splitting between the vibrational eigenenergies. On the other hand, when the anharmonicity parameters g_{iii} are distributed (diagonal disorder), a correlation coefficient must be assigned to describe this joint bivariate distribution, which in turn could lead to either correlated or anticorrelated broadening. Thus, while our treatment of the correlated inhomogeneous broadening of the two coupled vibrations using a joint Gaussian PDF parallels those of earlier works on the disordered aggregates,[14−17] the microscopic interpretation of our results is quite different.

Our experimental results indicate a strong positive correlation between the transition energies of the asymmetric and the symmetric vibrations and thus favor the case in which the solvent leads to a correlated distribution of anharmonicities for the local CO stretches. In a hexane solution, the RDC absorption line width is 2.6 cm^{-1} for both vibrations, and the broadening is dominated by reorientational relaxation and pure dephasing. The additional 6.7 and 12 cm^{-1} broadening of the line widths for *a* and *s* modes in a chloroform solution, respectively, is attributed to specific solvation effects on the vibrations. It is well-known that the metal carbonyl-stretching motions are very sensitive to the electron density of the metal atom due to $d_\pi-\pi^*$ bonding interactions. This interaction favors the donation of the electron density from the d orbitals of the central metal atom to the π antibonding (π^*) orbitals of the CO group[45] and ultimately modifies the vibronic potential.[46] RDC is a planar (d^8) coordination compound, and the Rh atom is exposed to solvent molecules in the primary solvation shell along the two axial positions. We suggest that the correlated broadening in this system arises from solvent density fluctuations from these axial directions, which modulate the electron density of the Rh atom. This in turn will modulate the strength of the $d_\pi-\pi^*$ bonding between Rh and CO groups in a manner that symmetrically influences the individual CO anharmonicities. The ensemble averaging of either effect will appear as a correlated distribution of the transition frequencies. Although different, these mechanisms do not exclude the intramolecular effects of CO coupling with a thermally populated Rh−C stretch that has been used to explain temperature-dependent dephasing.[46]

The model presented here also predicts unique signatures of correlation effects in the cross-peaks of 2D vibrational spectra. While the nature of the broadening of fundamental transitions is reflected in the diagonally elongated ellipticity of the diagonal peaks,[11,12] the correlation of fluctuations will be reflected in the shape of the cross-peaks. Strongly correlated broadening will appear as diagonally elongated cross-peaks, whereas anticorrelated broadening will appear as antidiagonally elongated cross-peaks. Uncorrelated fluctuations between the two transitions will lead to a symmetric cross-peak.

In summary, our analytical formalism of the total nonlinear third-order response function of two coupled vibrational motions using a correlated-broadening model is successful in reproducing the experimental features of 2D VDE signals such as decay and line width parameters, tilted contour shapes, and most importantly the frequency-dependent peak shift. Our results show the ability of 2D spectroscopies to quantitatively capture the correlated dynamics of coupled coordinates as well as provide insight into the microscopic picture of solute−solvent interactions. Although this model successfully reproduces all of the main features of the 2D signal, the assumption of inhomogeneous broadening is an oversimplification of the actual dynamics of the system. A more general approach to the study of room-temperature solvation would build correlation effects into solvation models that allow for arbitrary time scales for system−bath interactions. Such an approach using spectral densities for the energy gap between all pairs of states is the focus of ongoing work.

Acknowledgment. This work was supported by the National Science Foundation (Grant CHE-0079268). Additional support came from the U.S. Department of Energy (DE-FG02-99ER14988), the donors to the ACS-Petroleum Research Fund, and an award by the Research Corporation. N.D. thanks Jose Gonzales for his help with the FT-IR measurements. A.T. is a recipient of the David and Lucile Packard Foundation Fellowship.

References and Notes

(1) Mukamel, S. *Principles of Nonlinear Optical Spectroscopy*; Oxford University Press: New York, 1995.

(2) Fleming, G. R.; Cho, M. *Annu. Rev. Phys. Chem.* **1996**, *47*, 109.

(3) de Boeij, W. P.; Pshenichnikov, M. S.; Wiersma, D. A. *Annu. Rev. Phys. Chem.* **1998**, *49*, 99.

(4) Mukamel, S. *Annu. Rev. Phys. Chem.* **2000**, *51*, 691.

(5) Hamm, P.; Lim, M.; DeGrado, W. F.; Hochstrasser, R. M. *Proc. Natl. Acad. Sci. U.S.A.* **1999**, *96*, 2036.

(6) Woutersen, S.; Hamm, P. *J. Phys. Chem. B* **2000**, *104*, 11316.

(7) Golonzka, O.; Khalil, M.; Demirdöven, N.; Tokmakoff, A. *Phys. Rev. Lett.* **2001**, *86*, 2154.

(8) Merchant, K. A.; Thompson, D. E.; Fayer, M. D. *Phys. Rev. Lett.* **2001**, *86*, 3899.

(9) Hybl, J. D.; Albrecht, A. W.; Gallager-Faeder, S. M.; Jonas, D. M. *Chem. Phys. Lett.* **1998**, *297*, 307.

(10) Gallagher-Faeder, S. M.; Jonas, D. M. *J. Phys. Chem. A* **1999**, *103*, 10489.
(11) Okumura, K.; Tokmakoff, A.; Tanimura, Y. *Chem. Phys. Lett.* **1999**, *314*, 488.
(12) Tokmakoff, A. *J. Phys. Chem. A* **2000**, *104*, 4247.
(13) Zanni, M. T.; Asplund, M. C.; Hochstrasser, R. M. *J. Chem. Phys.* **2001**, *114*, 4579.
(14) Knapp, E. W. *Chem. Phys.* **1984**, *85*, 73.
(15) Domínguez-Adame, F. *Phys. Rev. B* **1995**, *51*, 12801.
(16) Domínguez-Adame, F.; Malyshev, V. A.; Rodríguez, A. *Chem. Phys.* **1999**, *244*, 351.
(17) Knoester, J. *J. Chem. Phys.* **1993**, *99*, 8466.
(18) Knoester, J. *J. Lumin.* **1994**, *58*, 107.
(19) Durrant, J. R.; Knoester, J.; Wiersma, D. A. *Chem. Phys. Lett.* **1994**, *222*, 450.
(20) Moll, J.; Daehne, S.; Durrant, J. R.; Wiersma, D. A. *J. Chem. Phys.* **1995**, *102*, 6362.
(21) Chernyak, V.; Mukamel, S. *Phys. Rev. Lett.* **1995**, *74*, 4895.
(22) Chernyak, V.; Wang, N.; Mukamel, S. *Phys. Rep.* **1995**, *263*, 213.
(23) Friedrich, J.; Haarer, D. *J. Chem. Phys.* **1983**, *79*, 1612.
(24) Sevian, H. M.; Skinner, J. L. *Theor. Chim. Acta* **1992**, *82*, 29.
(25) Dick, B.; Hochstrasser, R. M. *J. Chem. Phys.* **1983**, *78*, 3398.
(26) Cundiff, S. T. *Phys. Rev. A* **1994**, *49*, 3114.
(27) Cundiff, S. T.; Koch, M.; Knox, W. H.; Shah, J.; Stolz, W. *Phys. Rev. Lett.* **1996**, *77*, 1107.
(28) Erland, J.; Pantke, K.-H.; Mizeikis, V.; Lyssenko, V. G.; Hvam, J. M. *Phys. Rev. B* **1994**, *50*, 15047.
(29) Yang, M.; Fleming, G. R. *J. Chem. Phys.* **2000**, *113*, 2823.
(30) Piryatinski, A.; Tretiak, S.; Chernyak, V.; Mukamel, S. *J. Raman Spectrosc.* **2000**, *31*, 125.
(31) Tominaga, K.; Yoshihara, K. *Phys. Rev. A* **1996**, *55*, 831.
(32) Thompson, D. E.; Merchant, K. A.; Fayer, M. D. *Chem. Phys. Lett.* **2001**, *340*, 267.
(33) Thompson, D. E.; Merchant, K. A.; Fayer, M. D. *J. Chem. Phys.* **2001**, *115*, 317.
(34) Asplund, M. C.; Lim, M.; Hochstrasser, R. M. *Chem. Phys. Lett.* **2000**, *323*, 269.
(35) Golonzka, O.; Tokmakoff, A. *J. Chem. Phys.* **2001**, *115*, 297.
(36) Khalil, M.; Tokmakoff, A. *Chem. Phys.* **2001**, *266*, 213.
(37) Book, L. D.; Scherer, N. F. *J. Chem. Phys.* **1999**, *111*, 792.
(38) Koch, M.; Cundiff, S. T.; Knox, W. H.; Shah, J.; Stolz, W. *Solid State Commun.* **1999**, 533.
(39) Golonzka, O.; Khalil, M.; Demirdöven, N.; Tokmakoff, A. *J. Chem. Phys.* **2001**, submitted for publication.
(40) Beckerle, J. D.; Casassa, M. P.; Cavanagh, R. R.; Heilweil, E. J.; Stephenson, J. C. *Chem. Phys.* **1992**, *160*, 487.
(41) Kubo, R. *Adv. Chem. Phys.* **1969**, *15*, 101.
(42) Bury, K. V. *Statistical Models in Applied Sciences*, 1st ed.; John Wiley & Sons: New York, 1975.
(43) Yang, M. N.; Fleming, G. R. *J. Chem. Phys.* **1999**, *110*, 2983.
(44) Agarwal, R.; Yang, M.; Xu, Q.-H.; Fleming, R. G. *J. Phys. Chem. B* **2001**, *105*, 1887.
(45) Huheey, J. E.; Keiter, E. A.; Keiter, R. L. *Inorganic Chemistry: Principles of Structure and Reactivity*, 4th ed.; HarperCollins College Publishers: New York, 1993.
(46) Rector, K. D.; Fayer, M. D. *J. Chem. Phys.* **1998**, *108*, 1794.